

Bachelor thesis

Creating Models for Building Control

Jaroslav Tabaček



May 2014

supervisor: Ing. Eva Žáčková

Czech Technical University in Prague
Faculty of Electrical Engineering, Department of Control
Engineering

České vysoké učení technické v Praze
Fakulta elektrotechnická

katedra řídicí techniky

ZADÁNÍ BAKALÁŘSKÉ PRÁCE

Student: **Jaroslav Tabaček**

Studijní program: Kybernetika a robotika
Obor: Systémy a řízení

Název tématu: **Tvorba modelů pro řízení budov**

Pokyny pro vypracování:


1. Zoznámte sa s fyzikálnymi javmi v budovách so zameraním na modelovanie prenosu tepla.
2. Zostavte matematické modely rôznych zložitostí vybranej časti budovy na základe dát, ktoré dodá vedúci práce.
3. Navrhňte regulátor pre riadenie teploty v miestnosti.

Seznam odborné literatury:

- [1] M. Barták, Úvod do přenosových jevů pro inteligentní budovy. Praha: ČVUT, 2010. Dostupné na <www.ib.cvut.cz>.
- [2] C.P. Underwood, HVAC control systems: Modelling, analysis and design, E&FN SPON, London, 1999
- [3] S. Prívvara, Z. Váňa, E. Žáčková, J. Cigler: Building modeling: Selection of the most appropriate model for predictive control. Energy and Buildings, 2012 – Elsevier

Vedoucí: Ing. Eva Žáčková

Platnost zadání: do konce letního semestru 2014/2015


prof. Ing. Michael Šebek, DrSc.
vedoucí katedry




prof. Ing. Pavel Ripka, CSc.
děkan

V Praze dne 8. 1. 2014

Acknowledgement

I am grateful to my supervisors, Ing. Eva Žáčková and Ing. Matej Pčolka, whose guidance enabled me to develop an understanding of the subject. I would also like to thank my family who inspired, encouraged and fully supported me in every way. Lastly, I offer my regards to all of those who supported me in any respect during the completion of this thesis.

Declaration

I declare that I worked out the presented thesis independently and I quoted all used sources of information in accordance with Methodical instructions about ethical principles for writing academic thesis.

Prague, 22th May 2014



Jaroslav Tabaček

Abstrakt

Táto práca popisuje proces vytvárania matematického modelu budovy pre účely riadenia teploty a návrh regulátorov teploty na základe najlepšieho modelu.

Proces vytvárania takéhoto modelu zahŕňa popis základných mechanizmov prenosu tepla v budovách, vytváranie rôznych matematických model pomocou týchto mechanizmov, zjednodušovanie matematických modelov a identifikáciu neznámych parametrov. Identifikované modely sú testované na reálnych dátach a porovnávané s reálnym systémom. Týmto sa zistí presnosť matematických modelov, takže je možné vybrať ten najlepší.

Na základe týchto poznatkov je možné navrhnúť riešenie regulátora, ktoré spĺňa zadané požiadavky.

Kľúčové slová

identifikácia modelu; matematický model; stavové rovnice; model budovy; regulácia

Abstract

This thesis shows the process of creating a mathematical model of a building for purposes of temperature control. Further, it presents a controller design for temperature control based on the best model.

The process of model creation includes describing basic heat-transfer mechanisms in buildings, creating different mathematical models using these mechanisms, simplifying the mathematical models and identifying unknown parameters. The identified models are tested on real data and compared with a real system. This reveals accuracy of the mathematical models, thus making it possible to choose the best one.

Based on these findings, a controller design is developed, fulfilling the control requirements.

Keywords

model identification; mathematical model; state equations, building model, regulation

Contents

1. Introduction	1
2. Fundamental concepts	3
2.1. Conduction	3
2.2. Convection	4
2.3. Radiation	5
3. Modelling	7
3.1. Building description	7
3.1.1. Building A	7
3.1.2. Building B	8
3.2. Mathematical model	9
3.2.1. Building A	9
3.2.1.1. Heat transfer phenomena	9
3.2.1.2. State equations	10
3.2.2. Building B	12
4. Identification	14
4.1. Building A	15
4.2. Building B	16
4.2.1. Data	16
4.2.2. Parameters identification	19
5. Regulation	23
5.1. Supply fan	23
5.1.1. On-off controller	24
5.1.2. PI controller	25
5.2. Supply air temperature	26
5.2.1. PI controller	26
5.2.2. MPC-based controller	27
5.3. Conclusion on regulation	30
6. Conclusion	32
Prílohy	
A. Table of identified parameters for Building A	34
B. Table of identified parameters for Building B	35
Literatúra	36

Symbols

\dot{q}	Heat flux (W m^{-2}).
\dot{Q}	Heat flow (W).
T	Thermodynamic temperature (K).
U	Thermal conductivity of planar wall ($\text{W m}^{-2} \text{K}^{-1}$).
h_k	Convection heat transfer coefficient ($\text{W m}^{-2} \text{K}^{-1}$).
ϕ_{12}	Specific geometric constant (-).
σ	Stefan-Boltzmann constant ($\text{J s}^{-1} \text{m}^{-2} \text{K}^{-4}$).
ϵ	Emissivity of the surface (-).
k_{xy}	is product of coefficients C_{xy} , ϕ_{xy} , S_x , X and Y identify particular wall.
s_x	constant appropriate to the amount of heat flow added to the particular object (-).
h_x	Convection heat transfer coefficient for wall X ($\text{W m}^{-2} \text{K}^{-1}$).
r_x	Product of coefficients S , h_k .
p_x	Constant appropriate to the amount of heat flow added to the ceiling (-).
\dot{m}_w	Mass flow rate of the supply water (kg s^{-1}).
T_o	Outside temperature (K).
T_z	Zone temperature (K).
T_w	Temperature of the west-oriented wall (K).
T_e	Temperature of the east-oriented wall (K).
T_n	Temperature of the north-oriented wall (K).
T_s	Temperature of the south-oriented wall (K).
T_f	Temperature of the floor (K).
T_c	Temperature of the ceiling (K).
T_{SW}	Supply water temperature (K).
T_R	Return water temperature (K).
\dot{Q}_S	Solar radiation (W).
\dot{m}	Mass flow rate of the supply fan (kg s^{-1}).
T_O	Outside temperature (K).
T_Z	Zone temperature (K).
T_W	Temperature in the west-oriented office (K).
T_E	Temperature in the east-oriented office (K).
T_{COR}	Temperature in the corridor (K).
T_S	Temperature of supply air (K).

1. Introduction

In recent years, Heating, Ventilation and Air Conditioning (HVAC) systems integrated into building automation systems have become very popular. Their popularity results from their ability to quickly set and retain demanded temperature by using various sensors in combination with a sophisticated feedback-control system.

In order to study the system performance at the design stage, it is necessary to obtain approximate mathematical models for the components of the system. In addition, efficient control strategies play an essential role in developing improved energy control systems for buildings. The most important criteria for designing HVAC plants are energy efficiency and indoor climate conditions. An adequate combination of these two criteria demand gives the proper control of the plant [1].

Inefficiency in the building technologies, particularly in operating the HVAC systems, causes a significant part of the energy consumed by the building to be wasted. Part of the reason is that HVAC systems are operated on the basis of a pre-designed schedule of zone-wise temperature set points that zonal PID (proportional integral derivative) controllers then try to maintain. To improve energy efficiency, there is a growing interest in developing techniques that compute control signals that minimize building-wide energy consumption. Such control techniques require a model of the transient thermal dynamics of the building that relates the control signals to the space temperature and humidity of each zone. A model of the transient thermal dynamics of a multi-zone building can be derived from energy and mass balance equations. An attempt to model all the relevant physical phenomena will lead to a set of coupled differential equations. Prediction using such a model is computationally demanding due to the complexity of the model. However, an important requirement of a dynamic model for use in real-time control is simplicity, since overly complex models with large state spaces will render them too slow for prediction in real-time. Therefore, one has to use simplified, i.e., reduced order, models. In such a model, the air in a zone is assumed to be well-mixed so that each zone is characterized by a single temperature [2].

There are several possibilities of operational control strategies associated with the HVAC system for meeting the peak load. The performance of the selected system under transient loading conditions varies depending on the complexity (number of control variables) of the designed control strategy [3]. Conventional HVAC control strategies are based on maintaining a certain temperature set point in each zone by varying the supply air flow rate at fixed supply air temperature [1, 4, 5].

Many control strategies have been implemented to improve dynamic behaviour of air-conditioning systems. Model based analysis and simulation of airflow control of AHU (Air Handling Unit) units using PI (proportional integral) controllers [6], multivariable control of indoor air quality in a direct expansion air-conditioning system [7] and control tuning of a simplified VAV (Variable Air Volume) system [8] have been studied. Also, cascade control algorithm and gain scheduling [9], analysis of different control schedules on EMCS (Energy Management and Control System) [10] and model predictive control [11] of air-handling units have been investigated. In other control strategies, fuzzy control optimized by genetic algorithms (GA) [12], using a combination of artificial neural fuzzy interface modelling and a PID controller [13] and developing an adaptive fuzzy

1. Introduction

controller based on GA [14] have been implemented on air-handling units. In addition, optimal control [15], proportional optimal control [16] and adaptive self-tuning PI control [17] are other control approaches used for HVAC systems [18].

In light of the above, the purpose of this thesis is to create the simplest model of the building possible without any significant precision loss. The thesis is to be also understood as an introduction to the problematic of developing mathematical models of buildings.

The first part of the thesis shortly describes the physical phenomena of heat transfer.

The core of the thesis is a discussion of two buildings in respect to the phenomena outlined in the first part. Further information about heat transfer physical phenomena can be found in [19] or [20].

There are two buildings discussed in this thesis. Each building is modelled with different approach of model creation. The more sophisticated approach to a model creation of one the buildings is presented in a case-study provided in [21].

To conclude this thesis, the design of several simple controllers for temperature control in one of the modelled buildings is described and discussed.

2. Fundamental concepts

To create a mathematical model that describes thermal energy exchanges in buildings, we need to understand the fundamentals of heat transfer. There is a total of three heat-transfer mechanisms: conduction, convection and radiation. These three mechanisms will be further discussed in the following sections.

2.1. Conduction

To start describing thermal energy exchange we need to introduce several physical phenomena. The first of them is the heat flux, \dot{q} (W/m²). Fourier [22] described the heat flux by the equation

$$\dot{q} = -\lambda \nabla T, \quad (1)$$

where λ (W m⁻¹ K⁻¹) is scalar thermal conductivity and T (K) represents temperature. This equation is called the Fourier's law in differential form. The next phenomenon is the heat flow \dot{Q} (W) and if we assume that $\dot{q} = \text{const}$, we can write

$$\dot{Q} = \dot{q} \cdot S, \quad (2)$$

where S (m²) is an area through which the heat flows.

The heat transfer by conduction occurs in substances with no or negligible motion. Therefore, can be this mechanism observed mostly in solid substances. This transmission exists due to the interaction between the molecules of the substance.

Therefore in basic buildings the conduction takes place only on the air-wall-air interface. In the model we will assume that the direction of the incoming and the outgoing heat flux is perpendicular to the area of a wall. This allow us to only consider one-dimensional conduction.

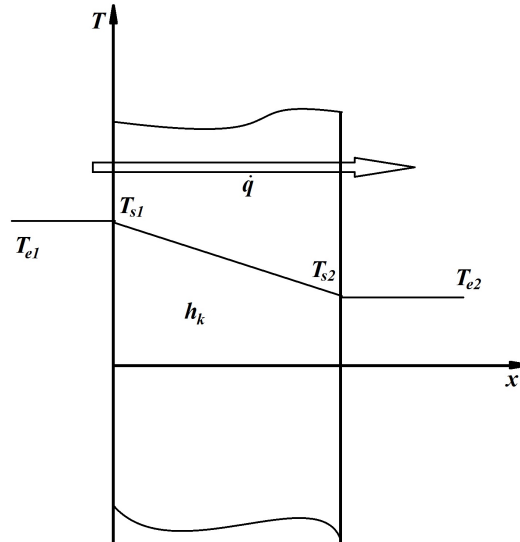


Figure 1. Conduction through a planar wall. T_{s1} and T_{s2} (K) represent the temperature of the surfaces, T_{e1} and T_{e2} (K) represent the temperature of the fluids, \dot{q} (W/m^2) represents the heat flux and h_k ($\text{W m}^{-2} \text{K}^{-1}$) is the conduction heat transfer coefficient.

With the approximations mentioned above, the conduction through the wall can be compared to the conduction through an infinite planar board. Then, as shown in [19], the conduction through a planar wall (Fig. 1) can be deduced from Fourier-Kirchhoff's equation and the result is

$$\dot{Q} = S U (T_s - T_e), \quad (3)$$

where S (m^2) is the area of the wall, U ($\text{W m}^{-2} \text{K}^{-1}$) is the thermal conductivity of the planar wall, T_s (K) is the temperature of the surface of the wall and T_e (K) is the temperature of the fluid.

2.2. Convection

Heat transfer by convection is generally associated with fluids and their motion. Convection can be divided in two groups: natural convection and forced convection.

Let us consider a plain wall surrounded by air with a different temperature. While energy transfer occurs, the density of the air is changing in consequence of changes in the air temperature. Therefore the air starts to move by itself. We call this phenomenon natural convection.

On the other hand, forced convection is caused by a fluid or a substance surrounded by fluid in motion. The velocity of the motion of the fluid in this case is generally much higher than the velocity caused by natural convection. The natural convection can be neglected in this case.

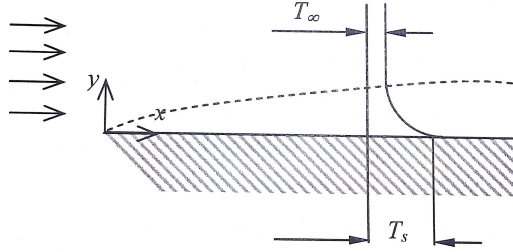


Figure 2. The onvection next to a wall. Taken from [19].

Convection heat flux of heat transfer between the wall and the fluid with constant velocity is

$$|\dot{q}| = h_k (T_s - T_\infty), \quad (4)$$

where h_k ($\text{W m}^{-2} \text{K}^{-1}$) is the convection heat transfer coefficient, T_s is the temperature of the surface of the wall and T_∞ is the temperature of the fluid at a theoretically infinite perpendicular distance from the wall.

Then the heat flow equation can be written as

$$|\dot{Q}| = S h_k (T_s - T_\infty), \quad (5)$$

where S (m^2) is the area of the wall.

Generally, the convection heat transfer coefficient is not constant but it depends on the temperature of the wall and the fluid. According to [19], the following simplified empirical relation can be used

$$h_k = c \sqrt[3]{\Delta T}, \quad (6)$$

where ΔT is the difference between the temperature of the wall and the fluid and c is the constant related to the position of the wall (horizontal, vertical; floor, roof) and its exact value is not important at this point.

2.3. Radiation

Unlike other heat-transfer mechanisms, radiation doesn't involve a material medium through which energy is transmitted. Rather, it is based on the existence of electromagnetic radiation. Of course, every object with temperature higher than absolute zero is a source of thermal radiation. But for our modelling purposes, we will not consider thermal radiation of gas. The threshold of the significance of thermal radiation is usually related to wavelength 100 nm. Therefore, we consider meaningful only radiation above this threshold. Another essential characteristic of radiation is its transmission in linear direction. So the angle of impact on the surface has to be studied as well.

The most important radiation type for this project is radiation between two surfaces (walls). The equation describing it, as shown in [19], is as follows:

$$\dot{Q} = C_{12} \phi_{12} S_1 \left[\left(\frac{T_1}{100} \right)^4 - \left(\frac{T_2}{100} \right)^4 \right], \quad (7)$$

where T_1 (K) and T_2 (K) are the temperatures of the surfaces, S_1 (m^2) is the area of the surface that is the source of radiation, ϕ_{12} (-) is the geometric constant that depends on the angle of impact of radiation and C_{12} can be written as

$$C_{12} = \epsilon_1 \epsilon_2 C_0, \quad (8)$$

2. *Fundamental concepts*

where ϵ (-) is the emissivity of the surface and $C_0 = \sigma 10^8$, where σ is the Stefan-Boltzmann constant.

3. Modelling

This chapter describes two different approaches for creating mathematical models for heat transfer in buildings. Each method will be applied on a different building. The choice of the method results from the type of data provided.

3.1. Building description

The buildings of interest are introduced separately in this section. For better orientation in the following text we will label these buildings as "Building A" and "Building B."

3.1.1. Building A

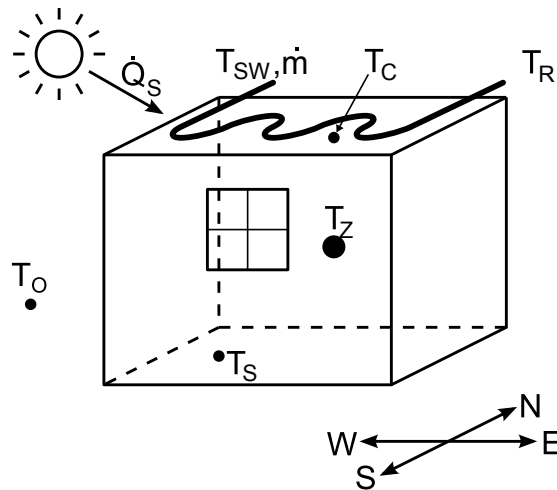


Figure 3. The Building A scheme. The picture taken from [23]

The first building taken into account is just a simulation model. It is modelled in the TRNSYS [24]. TRNSYS is a simulation environment for the transient simulation of thermal systems popular among a broad spectrum of engineers and researchers around the world. It can reliably simulate real environment behavior, therefore we will consider the model to be a satisfactory copy of a real building.

The building is simulated in a climate corresponding to the climate in Prague, Czech Republic. It consists of one room with dimensions $5 \times 5 \times 3$ m (Fig. 3). One window with the area of 3.75 m^2 is considered to be placed in the south-oriented wall. The metal pipes with the supply water in the ceiling wall are the main part of the Heating, Ventilation and Air Conditioning (HVAC) system used in the building.

The known thermal conductivities of the walls are shown in the Tab. 1.

3. Modelling

	U ($\text{W m}^{-2} \text{K}^{-1}$)
Side walls	0.668
Ceiling	1.246
Floor	2.564

Table 1. The thermal conductivity coefficients of the walls

Direct measurements of temperature of the south-oriented wall T_S , zone temperature T_Z and temperature of the return water T_R are available. The input controlled variables are the mass flow rate of the supply water \dot{m} and temperature of this water T_{SW} . The solar radiation \dot{Q}_S and outside temperature T_O are predictable system disturbances.

The building is considered to be "empty", that means that no additional radiation and convection sources are in the room.

3.1.2. Building B

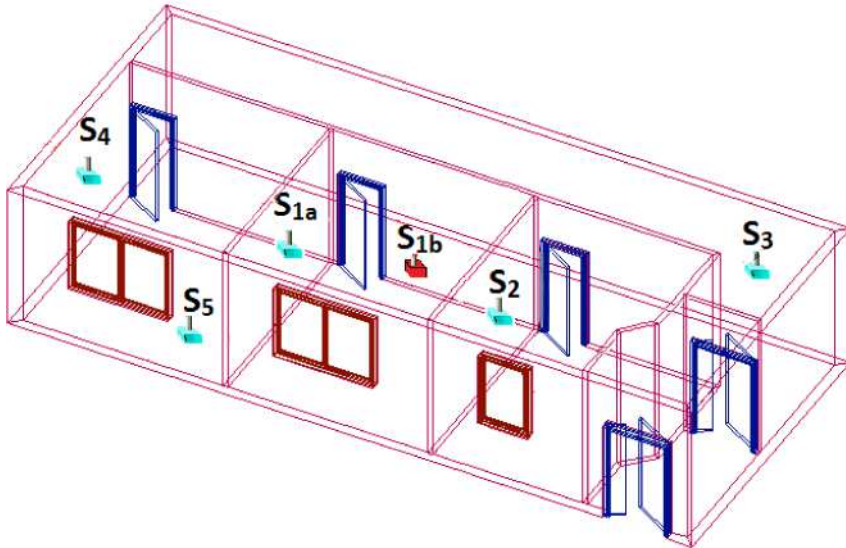


Figure 4. The Building B scheme. Devices denoted S_x are temperature sensors. The picture taken from [21]

The second building taken into account is part of the Lakeshore building at Michigan Technological University. In this thesis we will be interested only in one room in this building. The modelled room is a simple office with dimension $10.2 \times 8.5 \times 2.7$ m. It is surrounded by the corridor on the north side and two other offices on the west and the east side. There are also two double-layered windows facing south. The south-oriented wall that separates the room from the exterior is 0.7 m thick.

In the surrounding offices and the corridor, there are mounted temperature sensors with accuracy of $\pm 0.2^\circ\text{C}$ and humidity sensors. In the modelled room, there are two temperature sensors, humidity sensor and CO_2 sensor. One temperature sensor is situated near the window (S_{1b} in fig. 4) and it has accuracy $\pm 0.8^\circ\text{C}$. The other (S_{1a} in fig. 4) is of the same type as the temperature sensors in the rest of the rooms and is located next to the door. The CO_2 sensor measures in ppm units. Information about outside temperature is also provided.

The HVAC system with Water-Source Heat-Pumps is used to control temperature in the zones. For each zone there is a unique unit in the HVAC system and the controllers are of the on-off type. The temperature control in particular zones is provided by heated air which is delivered to the rooms by a supply fan with a constant mass flow rate of 0.52 kg s^{-1} . The supply fan is turned on only during business days between 4 AM and 6 PM.

3.2. Mathematical model

Many different approaches can be chosen to create a mathematical model for the temperature control. The best approach is the one in which the greatest possible number of provided data can be used and as few as possible of the model variables are neglected due to unmeasured values.

3.2.1. Building A

As state variables temperatures of each wall, temperature of the return water and the zone temperature were chosen.

Each state equation is written as

$$\frac{d}{dt}(T) = c \cdot d\dot{Q}, \quad (9)$$

where T (K) is the state variable (temperature of the wall or the return water), c is a constant that depends on the substance characteristics and $d\dot{Q}$ equals to the difference between incoming and outgoing heat flow.

3.2.1.1. Heat transfer phenomena

Conduction occurs between the outside temperature and the zone temperature with each wall as a barrier. The equation according to Eq. 3 is as follows:

$$\dot{Q} = S_x U_x (T_o - T_z). \quad (10)$$

The next type of conduction is conduction between heated water in the heating pipes in the ceiling and the ceiling itself. The equation for conduction heat flow in the return water temperature state equation is (for conduction heat flow in the ceiling see Eq. 16)

$$\dot{Q} = r_1 (T_c - T_R) + \dot{m}_w p_1 (T_{SW} - T_R), \quad (11)$$

where r_1 is the product of coefficients S , h_k and p_1 is a constant corresponding to the amount of heat flow added to the ceiling.

The heat flow from the solar radiation can be written as:

$$\dot{Q} = s_x \cdot \dot{Q}_S, \quad (12)$$

where s_x (-) is the constant corresponding to the amount of heat flow added to the particular object.

Then the radiation between each wall have to be considered. The equation according to Eq. 7

$$\dot{Q} = 10^{-8} k_{xy} (T_x^4 - T_y^4), \quad (13)$$

where k_{xy} is the product of coefficients C_{xy} , ϕ_{xy} , S_x .

3. Modelling

Convection occurs between the zone/outside temperature and each wall. The equation for heat flow by convection is determined by joining Eq. 5 and Eq. 6. The equation for temperatures of the walls is

$$|\dot{Q}| = S_x h_x (T_z - T_x)^{\frac{4}{3}}, \quad (14)$$

and for the zone temperature

$$|\dot{Q}| = S_x h_y (T_x - T_z)^{\frac{4}{3}}. \quad (15)$$

3.2.1.2. State equations

The state equations written with the assumptions made above are as follows

$$\begin{aligned} \frac{d}{dt}(T_z) &= c_1((3 S U + S_S U + S_C U + S_F U_F)(T_o - T_z) + \\ &\quad + s_1 \dot{Q}_S + \sum_i S_i h_i (T_i - T_z)^{\frac{4}{3}}), \\ \frac{d}{dt}(T_w) &= c_2(S h_1 (T_z - T_w)^{\frac{4}{3}} + S h_{11} (T_o - T_w)^{\frac{4}{3}} + \\ &\quad + s_2 \dot{Q}_S + 10^{-8} \sum_i k_{wi}(T_i^4 - T_w^4)), \\ \frac{d}{dt}(T_n) &= c_3(S h_2 (T_z - T_n)^{\frac{4}{3}} + S h_{22} (T_o - T_n)^{\frac{4}{3}} + \\ &\quad + s_3 \dot{Q}_S + 10^{-8} \sum_i k_{ni}(T_i^4 - T_n^4)), \\ \frac{d}{dt}(T_e) &= c_4(S h_3 (T_z - T_e)^{\frac{4}{3}} + S h_{33} (T_o - T_e)^{\frac{4}{3}} + \\ &\quad + s_4 \dot{Q}_S + 10^{-8} \sum_i k_{ei}(T_i^4 - T_e^4)), \\ \frac{d}{dt}(T_s) &= c_5(S_S h_4 (T_z - T_s)^{\frac{4}{3}} + S_S h_{44} (T_o - T_s)^{\frac{4}{3}} + \\ &\quad + s_5 \dot{Q}_S + 10^{-8} \sum_i k_{si}(T_i^4 - T_s^4)), \\ \frac{d}{dt}(T_c) &= c_6(S_C h_5 (T_z - T_c)^{\frac{4}{3}} + S_C h_{55} (T_o - T_c)^{\frac{4}{3}} + s_6 \dot{Q}_S + \\ &\quad + 10^{-8} \sum_i k_{ci}(T_i^4 - T_c^4) + r_2 (T_R - T_c) + \dot{m}_w p_2 (T_{SW} - T_R)), \\ \frac{d}{dt}(T_f) &= c_7(S_F h_6 (T_z - T_f)^{\frac{4}{3}} + S_F h_{66} (T_o - T_f)^{\frac{4}{3}} + 10^{-8} \sum_i k_{fi}(T_i^4 - T_f^4)), \\ \frac{d}{dt}(T_R) &= c_8(r_1 (T_c - T_R) + \dot{m}_w p_1 (T_{SW} - T_R)), \end{aligned} \quad (16)$$

where $i = \{W, N, E, S, C, F\}$ except the letter of the wall for which the state equation is written.

The mathematical model written above has in total 65 unknown parameters. Identification of such system would be too complex. Therefore, the system needs to be simplified. This simplification has to be done without significant loss of the precision of the model.

At this point, the influence of the solar radiation is included in the equations for the zone temperature and each wall. The solar radiation mostly affects the ceiling and the

south-oriented wall, and radiation on the other walls is significantly lower so it can be neglected. Then there is the solar radiation on the ceiling. The amount of the heat flow incoming from heating pipes is much higher compared to this radiation and so the solar radiation can be neglected again. The only solar radiation left is the solar radiation on the south-oriented wall and the solar radiation through the window to the zone.

Now, there are still 61 parameters and it is still too many. Because only data for 4 states is available, to run identification at this point, the computer would have to estimate 4 states apart from 61 parameters. Therefore, these 4 unmeasurable states and the influence of the these state variables will be neglected in the following process. The form of the state equations is as follows

$$\begin{aligned}
 \frac{d}{dt}(T_z) &= c_1((3SU + S_S U + S_C U + S_F U_F)(T_o - T_z) + s_1 \dot{Q}_S + \\
 &\quad + S_S h_S (T_s - T_z)^{\frac{4}{3}} + S_C h_C (T_c - T_z)^{\frac{4}{3}}), \\
 \frac{d}{dt}(T_c) &= c_6(S_C h_5 (T_z - T_c)^{\frac{4}{3}} + 10^{-8} k_{cs}(T_s^4 - T_c^4) + r_2 (T_R - T_c) + \dot{m}_w p_2 (T_{SW} - T_R)), \\
 \frac{d}{dt}(T_s) &= c_5(S_S h_4 (T_z - T_s)^{\frac{4}{3}} + S_S h_{44} (T_o - T_s)^{\frac{4}{3}} + s_5 \dot{Q}_S + 10^{-8} k_{sc}(T_c^4 - T_s^4)), \\
 \frac{d}{dt}(T_R) &= c_8(r_1 (T_c - T_R) + \dot{m}_w p_1 (T_{SW} - T_R)). \tag{17}
 \end{aligned}$$

At this point, the number of the parameters will not be decreased. The only simplification is made by approximating convection heat transfer coefficients as linear, not depending on temperatures. The state equations after this change are

$$\begin{aligned}
 \frac{d}{dt}(T_z) &= c_1((3SU + S_S U + S_C U + S_F U_F)(T_o - T_z) + s_1 \dot{Q}_S + \\
 &\quad + S_S h_S (T_s - T_z) + S_C h_C (T_c - T_z)), \\
 \frac{d}{dt}(T_c) &= c_6(S_C h_5 (T_z - T_c) + 10^{-8} k_{cs}(T_s^4 - T_c^4) + r_2 (T_R - T_c) + \dot{m}_w p_2 (T_{SW} - T_R)), \\
 \frac{d}{dt}(T_s) &= c_5(S_S h_4 (T_z - T_s) + S_S h_{44} (T_o - T_s) + s_5 \dot{Q}_S + 10^{-8} k_{sc}(T_c^4 - T_s^4)), \\
 \frac{d}{dt}(T_R) &= c_8(r_1 (T_c - T_R) + \dot{m}_w p_1 (T_{SW} - T_R)). \tag{18}
 \end{aligned}$$

For purpose of this model the nonlinearity of convection heat transfer coefficients is returned back and all radiations are neglected. The state equations are

$$\begin{aligned}
 \frac{d}{dt}(T_z) &= c_1((3SU + S_S U + S_C U + S_F U_F)(T_o - T_z) + s_1 \dot{Q}_S + \\
 &\quad + S_S h_S (T_s - T_z) + S_C h_C (T_c - T_z)), \\
 \frac{d}{dt}(T_c) &= c_6(S_C h_5 (T_z - T_c)^{\frac{4}{3}} + r_2 (T_R - T_c) + \dot{m}_w p_2 (T_{SW} - T_R)), \\
 \frac{d}{dt}(T_s) &= c_5(S_S h_4 (T_z - T_s)^{\frac{4}{3}} + S_S h_{44} (T_o - T_s)^{\frac{4}{3}} + s_5 \dot{Q}_S), \\
 \frac{d}{dt}(T_R) &= c_8(r_1 (T_c - T_R) + \dot{m}_w p_1 (T_{SW} - T_R)). \tag{19}
 \end{aligned}$$

The last approximation is made by neglecting all radiations and nonlinearities of convection heat transfer coefficients. So the final model is linear. Linear model state

3. Modelling

equations are:

$$\begin{aligned}
\frac{d}{dt}(T_z) &= c_1((3S_U + S_S U + S_C U + S_F U_F)(T_o - T_z) + s_1 \dot{Q}_S + \\
&\quad + S_S h_S (T_s - T_z) + S_C h_C (T_c - T_z)), \\
\frac{d}{dt}(T_c) &= c_6(S_C h_5 (T_z - T_c) + r_2 (T_R - T_c) + \dot{m}_w p_2 (T_{SW} - T_R)), \\
\frac{d}{dt}(T_s) &= c_5(S_S h_4 (T_z - T_s) + S_S h_{44} (T_o - T_s) + s_5 \dot{Q}_S), \\
\frac{d}{dt}(T_R) &= c_8(r_1 (T_c - T_R) + \dot{m}_w p_1 (T_{SW} - T_R)). \tag{20}
\end{aligned}$$

3.2.2. Building B

In this case, the model will be created based on the simple and intuitive equation:

$$V \cdot T(k+1) = V' \cdot T(k) + \sum_i V_i \cdot T_i(k), \tag{21}$$

where V (m^3), T (K) are the volume and temperature of the room, respectively, and V_i (m^3), T_i (K) represent the volume and temperature of air flowing from outside of the room. The relation between volumes is as follows

$$V = V' + \sum_i V_i. \tag{22}$$

Let us call Eq. 21 the mixed air equation. All that needs to be done now is to identify the external sources of the air that flows into the room.

The most significant one is obviously the hot air from the HVAC system that is accelerated by the supply fan. The mixed air equation can be written as:

$$V \cdot T(k+1) = V' \cdot T(k) + V_F \cdot T_F(k), \tag{23}$$

where V_F (m^3), T_F (K) are the volume and temperature of the air supplied by the supply fan. The problem is that the data for these particular variables are not provided. On the other hand, the data for the mass flow \dot{m} (kg s^{-1}) of the supply fan and the temperature of hot air from the HVAC system unit T_S (K) are available. Then the volume of the air flowing from the supply fan is:

$$V_F = \dot{m}(k) \cdot \frac{h}{\rho}, \tag{24}$$

where h (s) is the sampling period and ρ (kg m^{-3}) is density of the heated air. Because the hot air from the HVAC system unit is mixed with the room-temperature air on its way to the supply fan, in the ideal case the following equation can be written:

$$T_F(k) = T_S(k) - T_Z(k), \tag{25}$$

where T_Z (K) is the temperature in the zone (room). Summing up what has been discussed above we get the first model of the room:

$$T_Z(k+1) = \frac{V'}{V} T_Z(k) + \frac{h}{V \rho} \dot{m}(k) (T_S(k) - T_Z(k)). \tag{26}$$

The density of the air, of course, varies in time as the consequence of the changes in temperature and pressure of the heated air. In this case, the change of the pressure

is negligible in the considered temperature range. Therefore, we will consider it to be constant.

To improve the model we add the influence of the air in the corridor and the outside air and also sum the constants to one in front of each variable:

$$T_Z(k+1) = b_1 T_Z(k) + b_2 \dot{m}(k) (T_S(k) - T_Z(k)) + b_3 T_O(k) + b_4 T_{COR}(k), \quad (27)$$

where T_O (K), T_{COR} (K) are the outside temperature and the temperature in the corridor, respectively. Finally, the impact of temperatures of the air in the offices next to the room of interest are taken into account:

$$T_Z(k+1) = b_1 T_Z(k) + b_2 \dot{m}(k) (T_S(k) - T_Z(k)) + b_3 T_O(k) + b_4 T_{COR}(k) + b_5 T_E(k) + b_6 T_W(k), \quad (28)$$

where T_E is the temperature of the air in the east office and T_W represents temperature in the west office.

The last improvement is the increase of the system order up to the second. We will also increase the order of other variables of the system. The final model of the system is:

$$T_Z(k+1) = b_1 T_Z(k) + b_2 T_Z(k-1) + b_3 \dot{m}(k) (T_S(k) - T_Z(k)) + b_4 T_O(k) + b_5 T_{COR}(k) + b_6 T_E(k) + b_7 T_W(k) + b_8 T_O(k-1) + b_9 T_{COR}(k-1) + b_{10} T_E(k-1) + b_{11} T_W(k-1). \quad (29)$$

4. Identification

The process of estimating specific values of the parameters of the above mentioned mathematical models will be discussed in this chapter. It includes editing provided raw data and using algorithms to find parameter values of mathematical models that would fit the edited data. All data pre-processing, parameters identification and comparing have been done using Matlab [25].

The pseudocode in the Figure 4 roughly describes process of identification performed in Matlab [25]. The function *modelStructure* defines a state-space model. The function *greyboxModel* labels Matlab function *idgrey* in the case of a linear model or *idnlgrey* in the case of a nonlinear model. These functions create a grey-box model with identifiable parameters. The *parameters* in the function specify initial values of the parameters of the model. The creation of *model* is followed by restricting the model parameters to be greater than or equal to zero. This action has to be made due to Matlab's identification algorithms tendency to assign negative value to some parameters. However, if you look at the proposed mathematical models in Chapter 3, the constants in front of the variables can gain only positive value or zero.

The next step is loading the data that *model* is identified from. Afterwards the function *estimateModel* representing the Matlab function *pem* (Prediction error estimate for linear or nonlinear model) is applied. This function uses various algorithms to determine values of the model parameters in order to achieve the best possible fit between the model output and the provided data.

```
function modelStructure(parametersVector, samplingPeriod){...}

model = create greyboxModel(modelStructure, parameters);

model.Parameters.Minimum = 0;

testdata = load(data);
system = create estimateModel(testdata, model);
```

Figure 5. Pseudocode of identification process.

Accuracy of the models is verified by Matlab function *compare*. Inputs to this function are system and data on which the model should be tested and compared with. Outputs of *compare* function are the system response, initial states and the fit value. The fit value determines how accurate is the system response compared to the output data and evaluates this accuracy in percentage. The following expression shows how the fit value is calculated [25]

$$f = 100 \left(1 - \frac{|y - \hat{y}|}{y - \text{mean}(y)} \right) \quad (\%), \quad (30)$$

where y , \hat{y} represent data outputs and model response, respectively. We will further consider fit value to be reliable parameter for comparing models accuracy.

4.1. Building A

In this case, the model structure was defined in continuous-time state equations. The function *greyboxModel* in the pseudocode in Fig. 4 represents Matlab function *idnlgrey* mentioned above. In this section are shown the results of the identification procedure.

The accuracy of each output for each model expressed by fit value is shown in the following table.

Output	T_Z	T_C	T_S	T_R
Linear model (%)	71.85	78.83	63.90	81.58
Model with nonlinear coefficients (%)	72.63	76.25	66.21	80.95
Model with radiation (%)	74.63	79.32	59.52	82.35
Complete model (%)	74.56	77.92	63.93	81.63

Table 2. Comparison of the model accuracies based on the fit values.

The particular values of the identified parameters are shown in Appendix A.

In the next figure, one can see the differences between the linear model and the models with added particular nonlinearities. Also, if we compare this figure and Tab. 4.1, it can be seen how reliable are the fit values in evaluating accuracy of models.

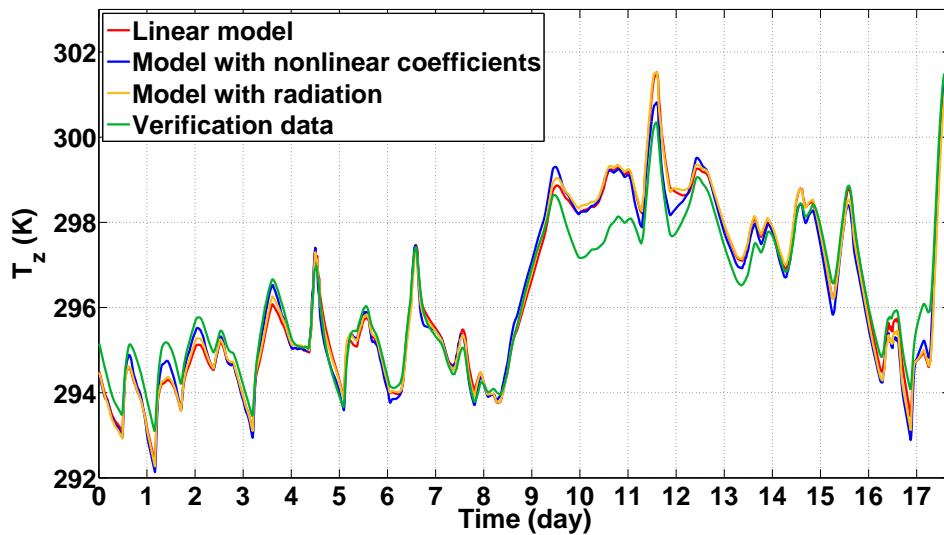


Figure 6. Comparison of models' responses and verification data for the temperature T_z .

The following figure shows the final comparison of the most significant identified models for the temperature in the zone.

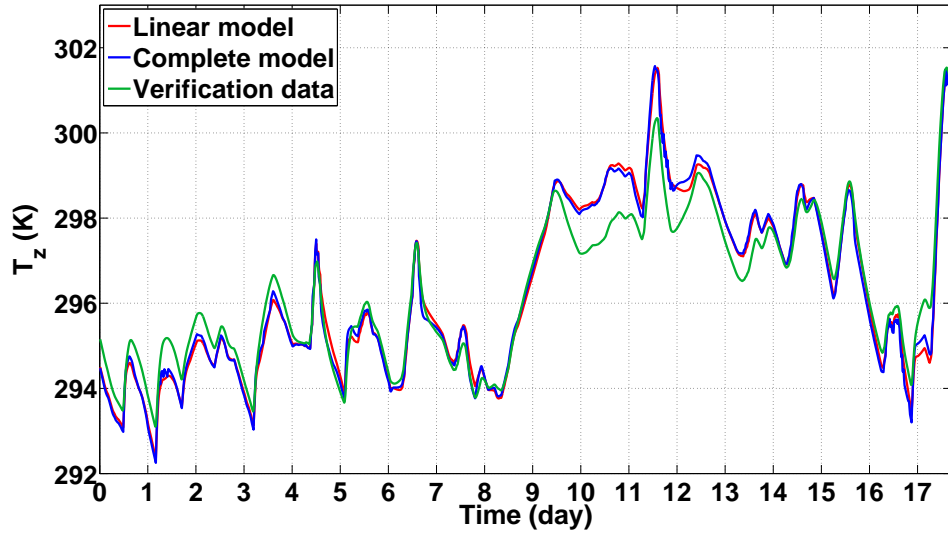


Figure 7. Comparison of models' responses and verification data for the temperature T_z .

The whole provided dataset consisted from 7801 samples. The data did not have to be pre-processed in any way. All models were identified on data range from 1st to 3500th sample. Each model was compared on dataset from 4000th to 7000th sample. The previous figures do not show the entire comparison range due to better view of differences between models. They show only about 1700 samples.

4.2. Building B

The provided data for Building B needed to be analysed before the identification procedure. The data did not come from simulations, therefore some sensors' sensitivity appears in some of them. This problem is further discussed in the following subsection.

After this issue is solved, the identification of the parameters can be initiated.

4.2.1. Data

As mentioned in Section 3.1.2, temperature data from outside, each zone, heated air and mass flow data of supply fan were available. These data were measured in 14-days period from 11th January 2013 to 24th January 2013 with a 60 seconds sampling period. The data of the indoor temperatures are shown in the following figure.

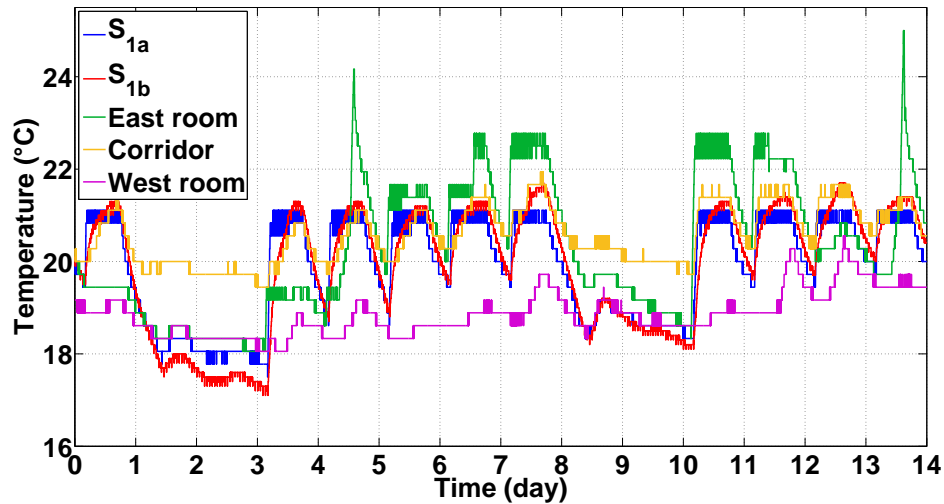


Figure 8. Provided data from all of the room sensors.

As seen in the figure above, some data needed to be smoothed. This had to be done for the data taken from room temperature sensors and outside temperature sensor, because of their sensitivity. Data acquired for supply fan mass flow didn't have to be filtered. Filtering the supply air temperature is debatable.

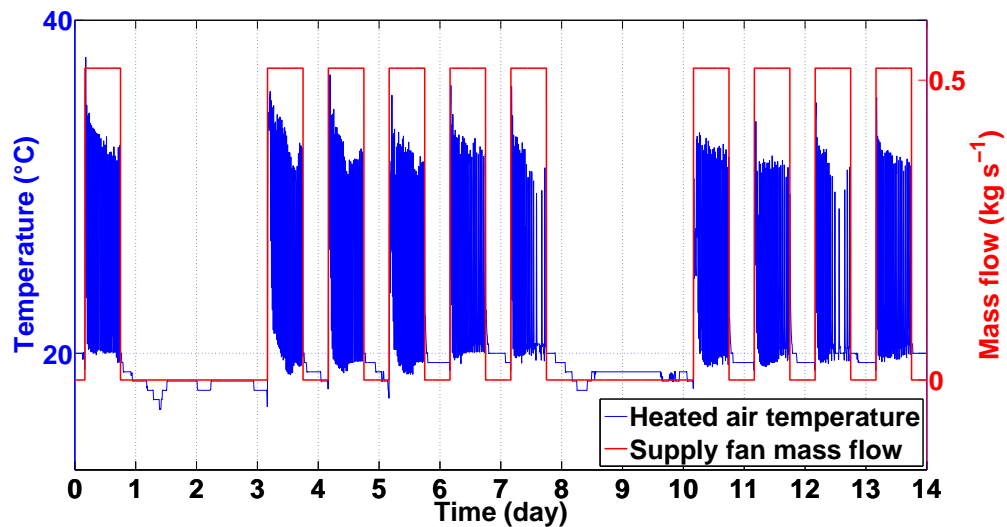


Figure 9. Provided data from heating system.

In fact there was no volatility in the data caused by the sensitivity of sensor, but data indicated changes on high frequency. We used unfiltered data as well as filtered data and will compare the results. The next thing to notice is turning on the heating and supply fan in the office only on business days.

The sampling period of raw data is as mentioned before 60 seconds. We need to realise that we are dealing with creating model for heat transfer in room where the changes are very slow. Therefore 60 seconds sampling period means too much unnecessary data

4. Identification

that could bring more confusion for identification because of more noise from sensors. We decided to resample data to 10 minutes sampling period.

The first step in the data pre-processing process was resampling the data. The resampling was done by simple script written in Matlab. Each sample in new (10 minutes) data represents arithmetic average of 10 successive samples in old (60 seconds) data. All data were resampled. The data that indicated temperatures in degree Celsius were converted to Kelvin units due to the compatibility with the assumptions made in Subsection 3.2.2.

To simplify entitling the data we denote data inputs and outputs as seen in the table:

T_{Z1}	Temperature in the room of interest from sensor S_{1a} (K)
T_Z	Temperature in the room of interest from sensor S_{1b} (K)
T_E	Temperature in the east room (K)
T_W	Temperature in the west room (K)
T_{COR}	Temperature in the corridor (K)
T_O	Outside temperature (K)
T_S	Temperature of supply air (K)
\dot{m}	Supply fan's mass flow (kg s^{-1})

Table 3. Denoting the data.

After resampling were some of the data filtered. For T_{Z1} , T_Z , T_E , T_W , T_{COR} and T_O (see Tab. 3) was used Matlab function *smooth* with robust version of locally weighted scatterplot smoothing filter (lowess) option with 27 samples span. Locally weighted scatterplot smoothing filter is a method which uses locally weighted linear regression to smooth data.

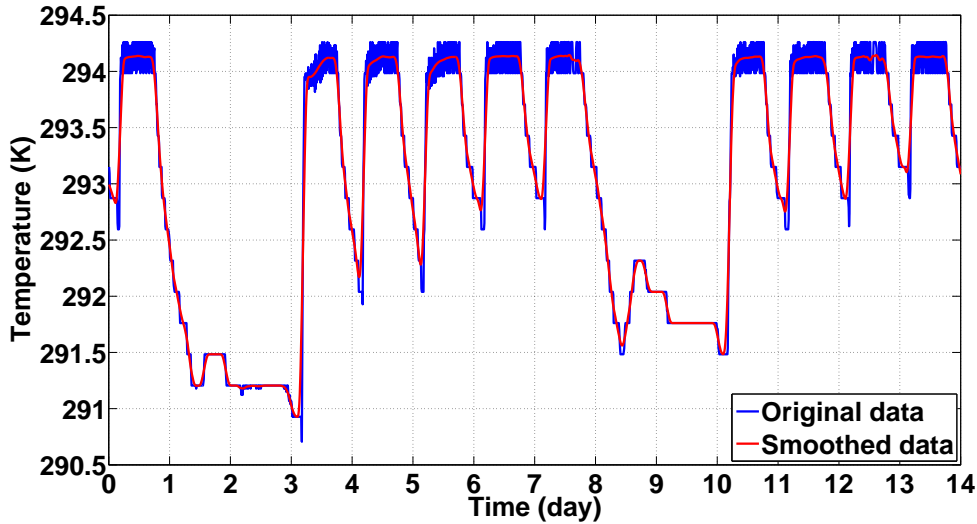


Figure 10. Result of applying "lowess" smoothing filter on the data for temperature T_{Z1} .

T_S was filtered also with Matlab function "smooth" but with moving average filter option and 3 samples span.

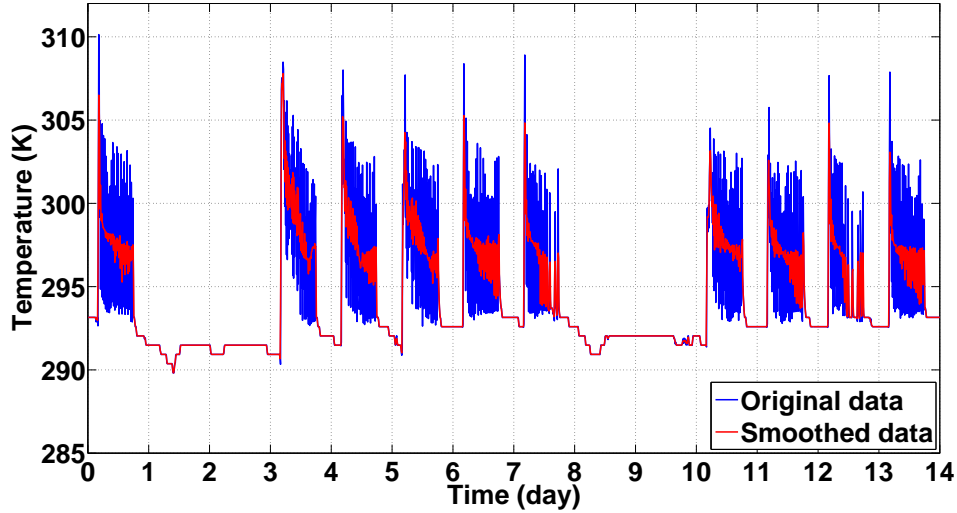


Figure 11. Result of applying moving average smoothing filter on the data for temperature T_S .

Example of the result of the data filtering can be seen in Fig. 10. All sensor sensitivity from outside temperature and room temperature sensors was successfully removed. Data length shrank from original 20160 samples to 2016 samples.

A high-frequency changes from heated air temperature data were partially removed. These data should not be smoothed entirely, because of loss of information about the most of the temperature settings during day.

4.2.2. Parameters identification

The models for this building were structured in discrete-time state-space matrices. The function *geryboxModel* in pseudocode in Fig. 4 represents Matlab's function *idgrey* mentioned at the beginning of this chapter.

To preserve mathematical model linearity let us denote expression $\dot{m}(k)(T_S(k) - T_Z(k))$ as $\dot{Q}(k)$ and consider this term as one input. That means $Q(k)$ is calculated before passing to identification algorithms.

The models were identified from the simplest structures to more complex ones. The final parameters for the variables from the simple models were set as the initial parameters for the more complicated models. The purpose of this process is simple. Matlab algorithms for parameters fitting are very sensitive on initial values of parameters. As the models get more complex, the algorithms tend not to converge to good results.

First thing to do was to transform Eq. 29 to state-space matrices. The feedthrough matrix D was always a zero matrix and the output matrix C was always set to one at state variable T'_Z . The system matrix A and input matrix B varied depending on the complexity of model. The full model described by Eq. 29 was rewritten into state-space structure as follows

4. Identification

$$\mathbf{x}(k+1) = \begin{bmatrix} 0 & 1 & 0 & 0 & 0 & 0 \\ b_1 & b_2 & b_3 & b_4 & b_5 & b_6 \\ 0 & 0 & 0 & 0 & 0 & 0 \\ 0 & 0 & 0 & 0 & 0 & 0 \\ 0 & 0 & 0 & 0 & 0 & 0 \\ 0 & 0 & 0 & 0 & 0 & 0 \end{bmatrix} \mathbf{x}(k) + \begin{bmatrix} 0 & 0 & 0 & 0 & 0 \\ b_7 & b_8 & b_9 & b_{10} & b_{11} \\ 1 & 0 & 0 & 0 & 0 \\ 0 & 1 & 0 & 0 & 0 \\ 0 & 0 & 1 & 0 & 0 \\ 0 & 0 & 0 & 1 & 0 \end{bmatrix} \cdot \mathbf{u}(k), \quad (31)$$

where vectors $\mathbf{x}(k)$ and $\mathbf{u}(k)$ were

$$\begin{aligned} \mathbf{x}(k) &= [T_Z(k) \quad T'_Z(k) \quad T'_E(k) \quad T'_{COR}(k) \quad T'_W(k) \quad T'_O(k)]^T, \\ \mathbf{u}(k) &= [T_E(k) \quad T_{COR}(k) \quad T_W(k) \quad T_O(k) \quad \dot{Q}(k)]^T. \end{aligned} \quad (32)$$

We denoted this model as model 5. To define simpler models we started from the full model and we indicated which variable was present and which was not. Defining such models is described in the following table. The table also contains the results of the identification in form of the fit value.

Model	T_Z	T'_Z	T'_E	T'_{COR}	T'_W	T'_O	T_E	T_{COR}	T_W	T_O	\dot{Q}	f (%)
1	0	1	0	0	0	0	0	0	0	1	1	-2.24
2	0	1	0	0	0	0	1	1	1	1	1	53.53
3	1	1	0	0	0	1	0	0	0	1	1	5.87
4	1	1	0	1	0	1	0	1	0	1	1	66.54
5	1	1	1	1	1	1	1	1	1	1	1	67.19

Table 4. Defining model structures that are objects of identification. The zeros in the table indicate that the variable was not present in the model structure. On the other hand the ones indicate the variable was taken into account as seen in structure in Eq. 31 and Eq. 32

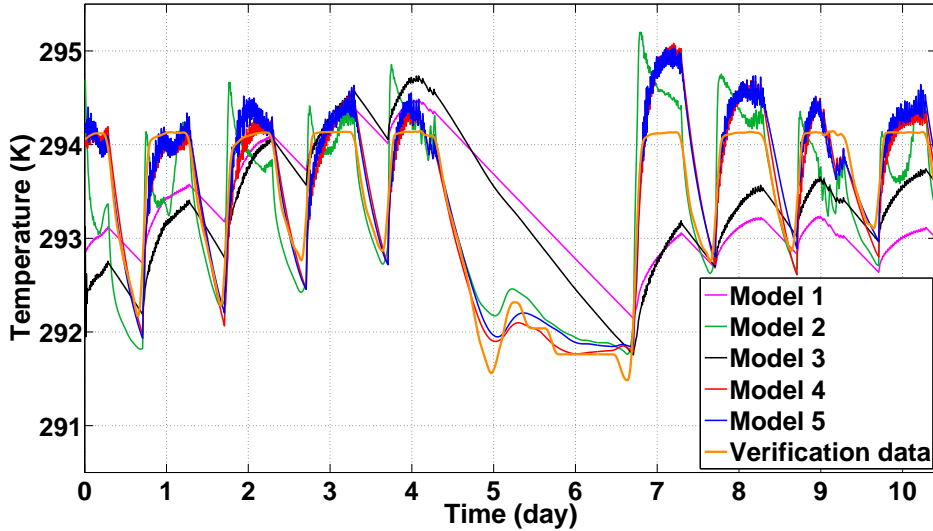


Figure 12. Comparison of responses of the models and real data.

All models mentioned above were identified from data with unprocessed temperature of heated air. That is the reason for plot not being smooth. We took the best model,

which was the full model and identified it from data partially filtered as described in Subsection 4.2.1. The result achieved fit value of 67.93 %. The following figure shows comparison of this model with the model with the same structure but identified on non-filtered data.

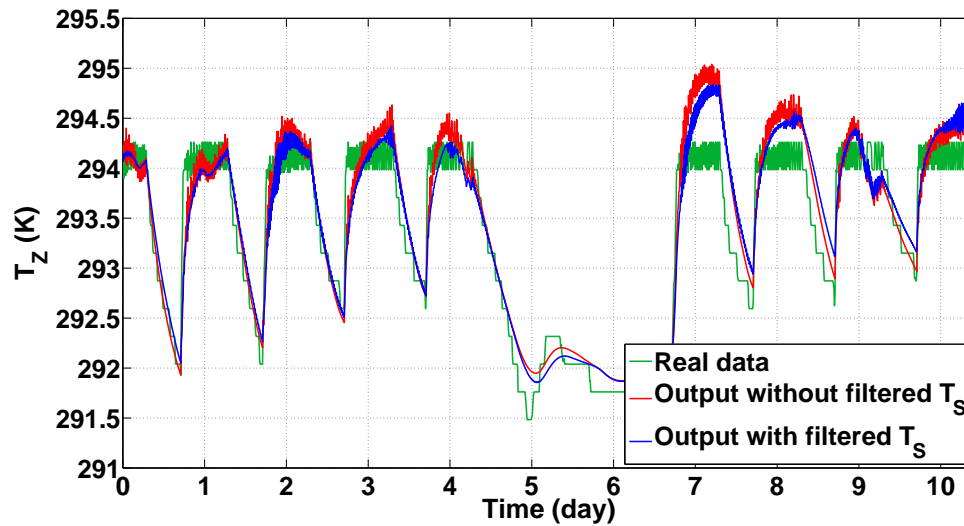


Figure 13. Comparison of model with the filtered and non-filtered temperature of heated air.

The last thing to do is to check if the model's behaviour corresponds to the reality. This test can be done by analysis of the step responses of the model. In the following figure are shown the independent step responses for each model input.

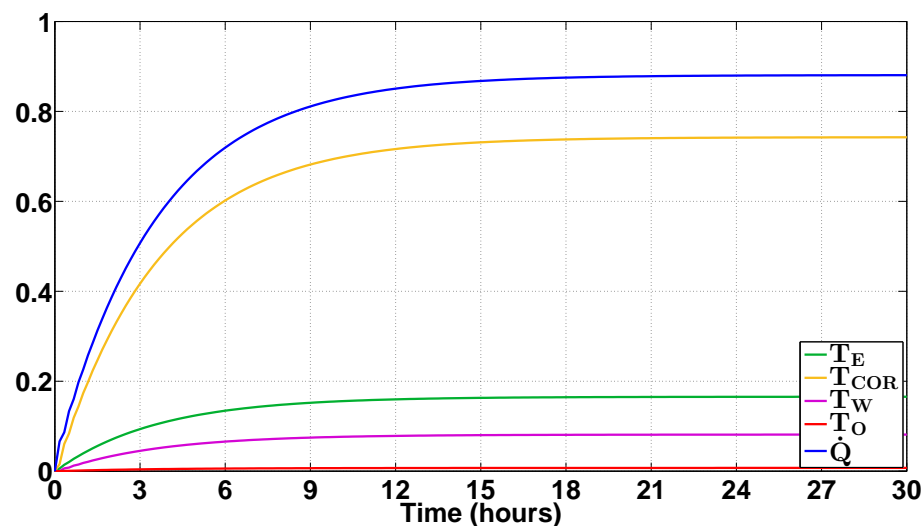


Figure 14. Step responses of the best identified model.

The settling time for all inputs is approximately 14 hours. The input reference is not reached for any input of the model. The most significant impact on the model has the input from the supply fan. The smallest steady state value has the step for

4. Identification

the outside temperature output. This behaviour is plausible considering that the wall is 0.7 m thick. On the other side, the walls between rooms are thinner, therefore the impact on the zone temperature is bigger for the temperatures in the west and the east room. The wall segregating the corridor from the room is similar to the ones between the rooms. Despite of this fact, the steady state is clearly smaller. This is probably caused by opening the door and the gap between the door frame and the door. The step responses coincide with the potential real system, hence the identification can be consider successful.

5. Regulation

The last part of this thesis describes the control system design. Since this process is similar for each building, we focus only on designing the control system for the Building B. This choice has also been made because as mentioned before the Building B is a real building.

The goal of the control system is to ensure the demanded scheduled temperature in the zone. The model on which basis we design and test controllers is the Model 5 described in Subsection 4.2.2.

Effectively, there are only one input to the model that can be influenced so the options are limited. This input (\dot{Q}) is proportional to $\dot{m}(k)(T_S(k) - T_Z(k))$ (see Subsection 4.2.2). All in all, we have three options of the control. We can either regulate the supply-fan mass flow, the heated air temperature or both at the same time.

All simulations were done using Simulink software [26].

5.1. Supply fan

In this section regulation of the zone temperature by controlling the mass flow of the supply fan is discussed. The hardware limitation allow us to set the controller into one of the three states (full power, half power, off). The currently used control system in the real building is using only two states (full power, off). Before we begin designing the controller, we need to ensure the appropriate setting of the temperature of the heated air.

To arrange simplicity, we calculated the heated air temperature as a function of the outside temperature.

$$T_S = aT_O + b, \quad (33)$$

where a, b are unknown constants. The constants were estimated by using the algorithm described by the following pseudocode:

```
data = sort {t_s,t_o} by t_s;

for i = 1 to data.length do {
t_s(i) = average(from t_s(i-5) to t_s(i+5));
t_o(i) = average(from t_o(i-5) to t_o(i+5));
}

{a,b} = linearRegression(t_s, t_o)
```

Figure 15. Pseudocode describing the process of identification of the coefficients in Eq 33.

The final equation characterizing the temperature of the heated air is as follows

$$T_S = -0.4663 \cdot T_O + 433.105 \quad (K). \quad (34)$$

5.1.1. On-off controller

The first controller to be designed is of the on-off (bang-bang) type. As the name of this controller hints, the mass flow can be either set on the maximum (0.52 kg s^{-1}) or turn off completely.

In the following figure, the scheme of this controller is shown.

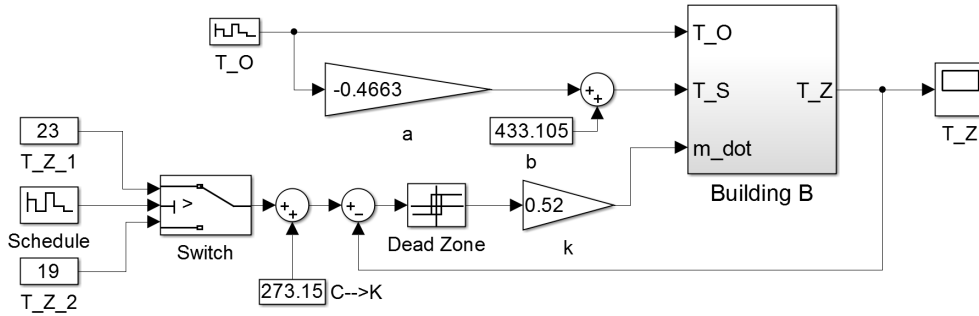


Figure 16. The Simulink model with the on-off controller.

The reference temperature in the figure is created by switching between two temperatures according to the schedule. The higher temperature is set at the working time, the lower temperature is set when no people are expected in the office.

This feedback control is completed with the *Dead Zone* block. The block preserves its previous output if the input is in the range between -0.2 and 0.2 . The output is zero if the input is below the range and it equals to one if the input is above the range. This restriction was done to minimize the oscillations near the reference threshold, therefore diminish the fast turning on and off the supply fan. With this configuration is the temperature in the room moving within the range of 0.4°C around the reference temperature. The simulation of this system is presented in the following figure.

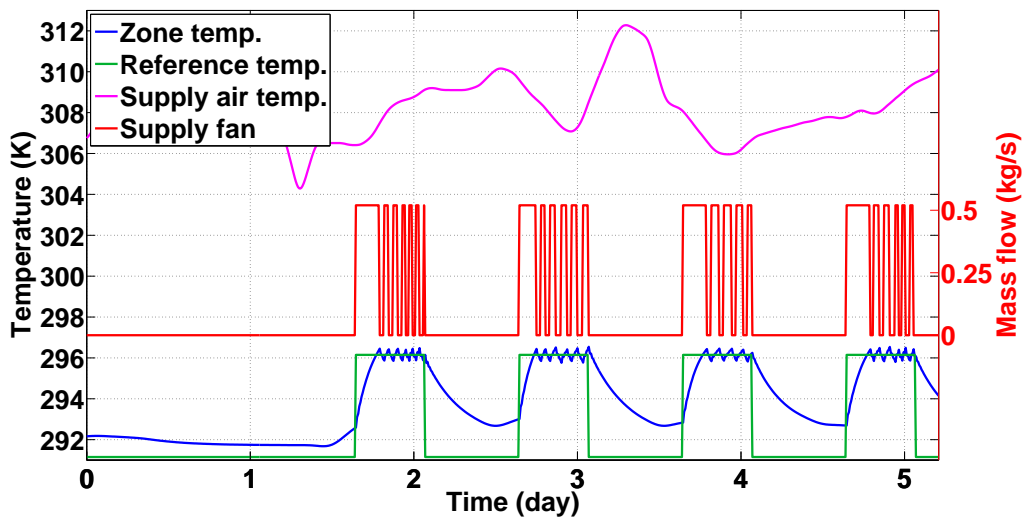


Figure 17. Response of the model with the on-off controller.

5.1.2. PI controller

The next controller for the supply fan mass flow utilise all the 3 states of setting of the supply fan. The 3 states are: full power (0.52 kg s^{-1}), half power (0.26 kg s^{-1}), off (0 kg s^{-1}). To make use of these settings we use PI (proportional integral) controller. To suppress the oscillations around the zero error we use the *Dead Zone* block. The scheme with the PI controller is shown in the following figure.

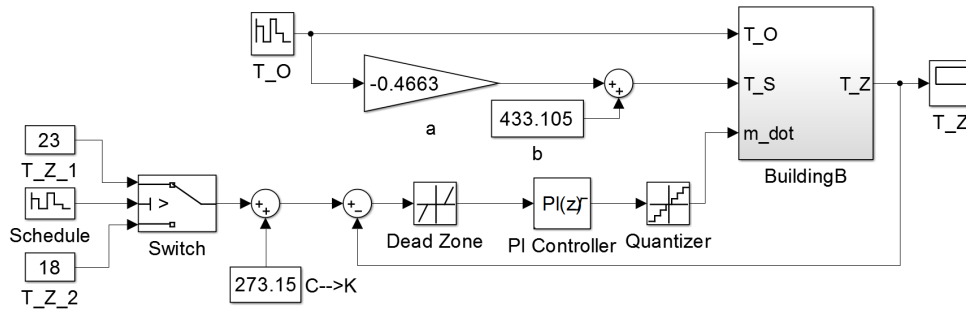


Figure 18. Simulink model with the quantized PI controller.

The PI controller was designed by the Root Locus method and further tuned using the simulink simulation. The transfer function of the designed controller is as follows

$$PI(z) = 0.255 \left(1 + \frac{0.0003 h}{z - 1} \right), \quad (35)$$

where h (s) is the sampling period of the system. In this case h equals to 600 s. Because of the limited input to the supply fan, the output of the PI controller was limited to the range from 0 to 0.52 with the clamping anti-windup method. The control action is further processed by the quantizer which quantizes with interval of 0.26 K.

The result of the functionality of this design is presented in the following figure.

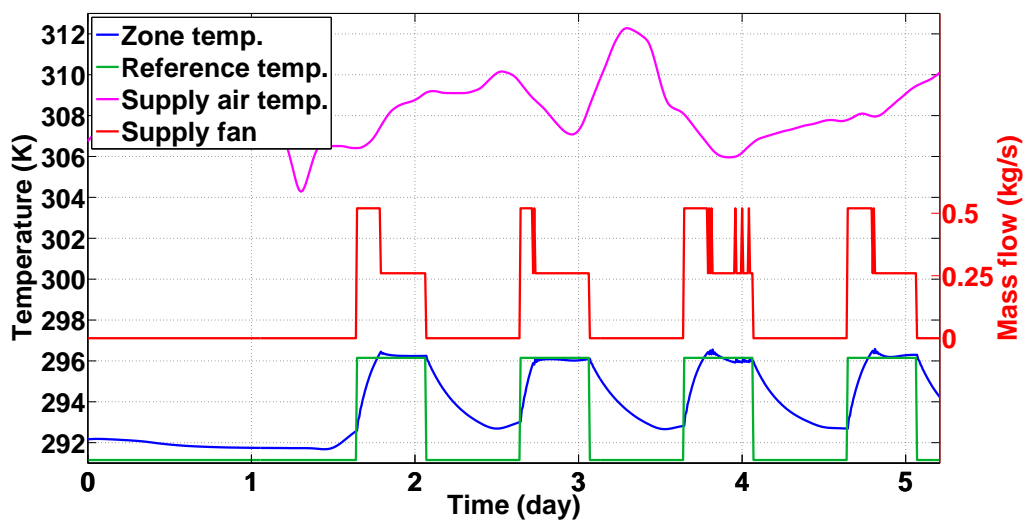


Figure 19. Response of the model with PI controller.

5.2. Supply air temperature

Compared to the control of the mass flow, the feedback control of the supply air temperature gives opportunity to set the temperature continuously. Therefore, the progress of the change of the zone temperature can be smoother. The range of the possible supply air temperature setting is between 10 and 40°C.

5.2.1. PI controller

The first used controller is again a PI controller. It was designed using the Root locus method and tuned using the simulation outputs. The final design is described by the following transfer function

$$PI(z) = 22.5 \left(1 + \frac{0.00018 h}{z - 1} \right), \quad (36)$$

where h (s) is the sampling period (600 s). The output of the controller is limited to the range from 10 to 40°C using the clamping anti-windup method. The scheme is presented in the next figure

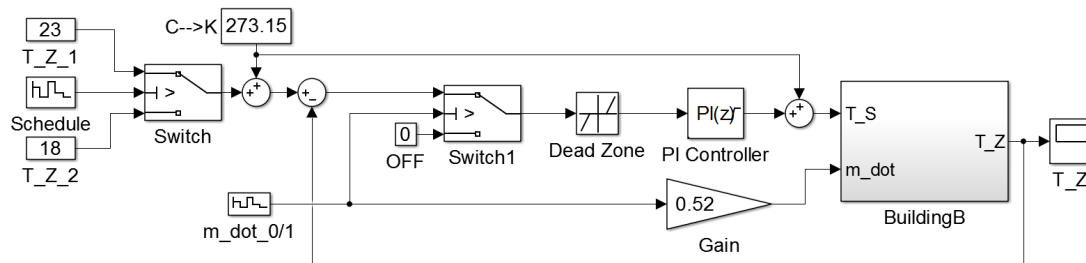


Figure 20. Simulink model with PI controller.

The supply fan is turned on during the working hours and the reference temperature is set with the same schedule. The *Dead Zone* block hold the previous output if the input is in range between -0.1 and 0.1. The purpose of the switch in front of the controller is to switch off setting the temperature if the supply fan is not working, because no heated air is blown into the room at that time. This could also save some energy. Last thing to mention is adding the constant on controller output. The function of this feature is to move zero to Kelvin scale, because the model is modelled to temperatures in Kelvin scale.

The simulation of this configuration is shown in the following figure.

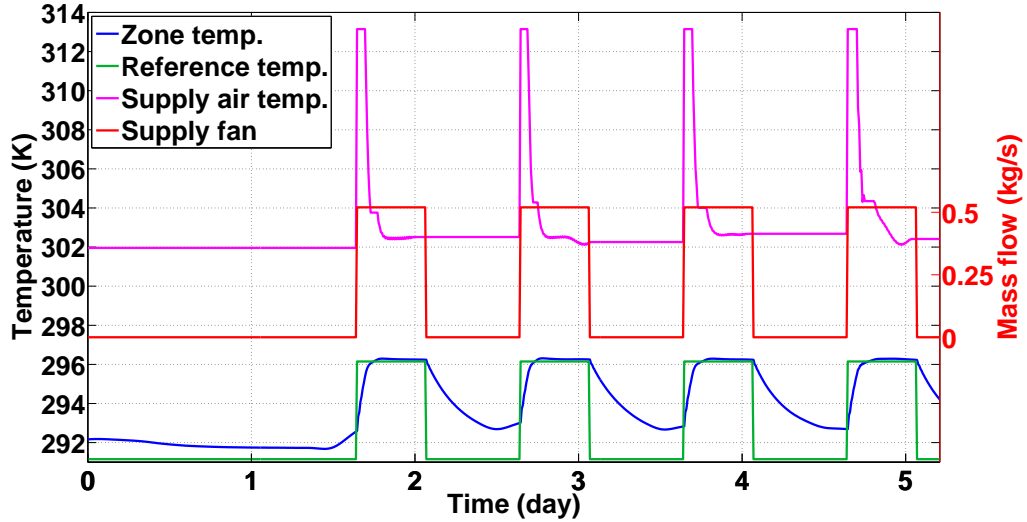


Figure 21. Response of the model with PI controller of the heated air temperature.

5.2.2. MPC-based controller

Model predictive control (MPC) is a control strategy in which the control action is obtained by minimizing, at each sample step, an open-loop cost function subject to constraints on the input amplitude and input moves. In the usual approach, the controller minimizes the distance between the predicted output trajectory and the desired output reference. The cost also includes a term that penalizes the thermal discomfort [27].

Compared to the other designed controllers, the MPC-based controller is provided with the information about the future changes in some of the model variables. This enables it to overcome the unnecessary overheating or underheating of the zone, therefore less energy is consumed.

Designing such sophisticated controller would exceed the focus of this thesis. Therefore we only used data generated by the model with configured MPC controller. Then we tried to find a relation that expresses how the supply air temperature depends on the other model variables and used this dependence as the design of the controller of the supply air temperature. This approach can also be used in buildings where the appropriate hardware or software for solving the optimization problem of MPC is not available.

The supply air temperature set by the MPC controller mostly depends on the future reference, the temperature in the zone and the output temperature. The final model of the supply air temperature that we decided to use is described by the following equation

5. Regulation

$$T_S(k+1) = \begin{bmatrix} a_1 & a_2 & \dots & a_{36} & a_{37} \end{bmatrix} \begin{bmatrix} T_Z(k) - T_R(k) \\ T_Z(k) - T_R(k+1) \\ \dots \\ T_Z(k) - T_R(k+35) \\ T_Z(k) - T_R(k+36) \end{bmatrix} + \begin{bmatrix} b_1 & b_2 & b_3 & b_4 \end{bmatrix} \begin{bmatrix} T_{O_{avg}}(k-36) \\ T_{O_{avg}}(k-18) \\ T_{O_{avg}}(k+18) \\ T_{O_{avg}}(k+36) \end{bmatrix} + cT_O(k) + d, \quad (37)$$

where d (K) is the constant approximating the influence of the neglected elements. $T_{O_{avg}}$ data represent 6 hours average of T_O data and were created by the following expression:

$$T_{O_{avg}}(k) = \frac{1}{73} \left(\sum_{i=-36}^{36} T_O(k+i) \right) \quad (38)$$

The future values would be substituted with weather forecast in the real case. The zone temperature and the reference are present in form of a subtraction because this correspond to the MPC cost function whose minimizer we approximate.

The identification of the parameters was done pursuant to process described in the beginning of Chapter 4 but without constraining the parameters.

In this system, the supply fan is turned on all the time. The described MPC-based controller functions only as the feedforward control of the system. This control is not sufficient and we would lost information about the disturbances in the zone. Therefore, the PI controller was added to the feedback loop and the outputs of this two controllers are summed up. The transfer function of the PI controller is following

$$PI(z) = 4.5 \left(1 + \frac{0.00005 h}{z-1} \right). \quad (39)$$

The scheme of the whole system is presented in the following figure.

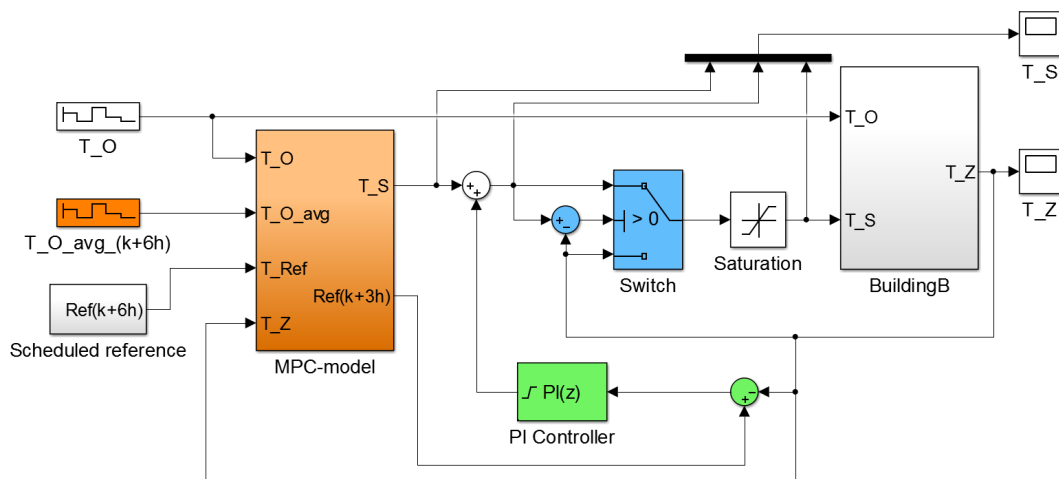


Figure 22. The Simulink model with the MPC-based control.

The blue-coloured part in the figure chooses the higher temperature from the temperature of the supply air and the zone temperature. This means that if the zone temperature is higher than the supply air temperature, the system circulates the zone temperature instead of cooling the zone with lower supply air temperature. The zone temperature decreases slower and this leads to saving the energy. The supply air temperature input to model is limited with *Saturation* block to range between 10 and 40°C.

The orange-coloured area labels the feedforward part with MPC-based controller and the green part represent the feedback control. The input to the PI controller is calculated from the future reference so it can follow the present reference instantly. The output of the PI controller is limited to the range between 0 and 10. The PI controller should not decrease the output of the MPC-based controller, hence the lower limit is zero. The upper limit is tuned to satisfy the maximum supply air temperature of the system.

This control scheme should not to follow the reference, but it is expected to continuously ensure the comfort temperature above the reference without the delay. The simulation of this system is shown in the next figure.

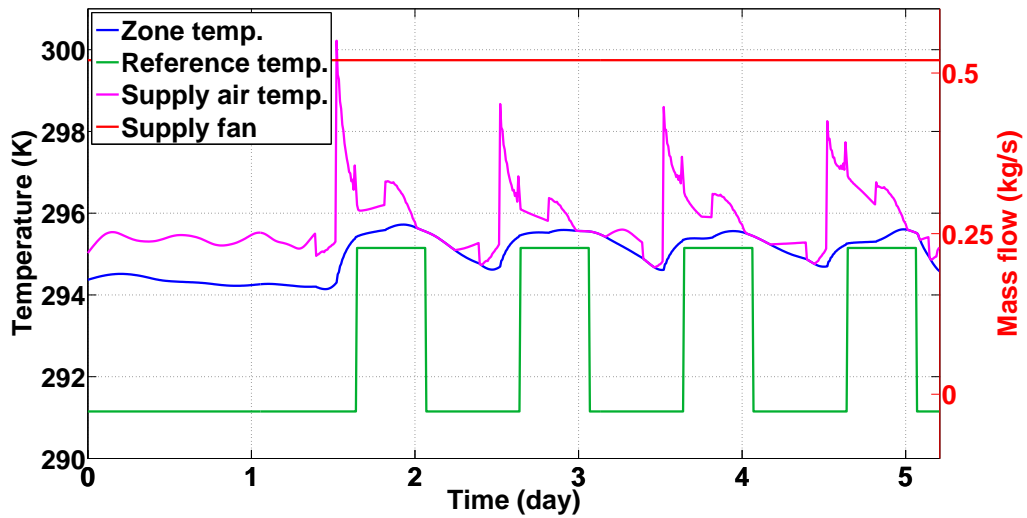


Figure 23. Response of the model with MPC-based control of the heated air temperature.

The next figure present the comparison of the value of the supply air temperature at different stages of the evaluation. The compared variables are: the feedforward control output, the feedback control output and the final temperature after comparing with the zone temperature. The graphic illustration of the compared stages is shown in Figure 22 (data synced by the T_S block).

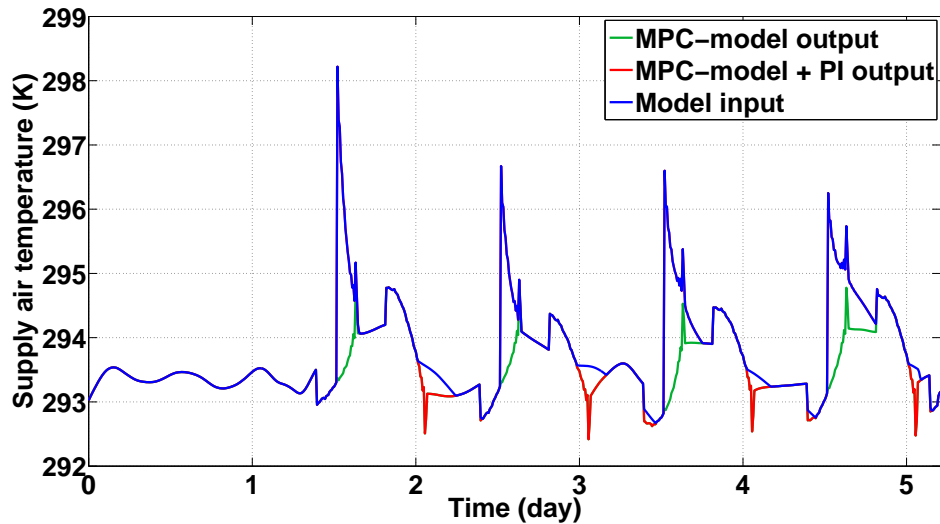


Figure 24. Comparison of the contributions to the value of the supply air temperature.

5.3. Conclusion on regulation

All of the controllers shown in this chapter were successfully designed and their functionality was tested on the simulations.

To choose the best one we compared them in respect of the total energy consumption (TE) and the amount of the underheating (UH).

The consumed energy depends on the heat exchange in the zone. For our purposes, we don't need the exact formula for evaluating the energy consumption. Instead, we use the following expression and we will consider it to be reliable.

$$TE = \sum_n \dot{m} (T_S - T_Z). \quad (40)$$

We define the underheating coefficient as the sum of the differences between the reference temperature and the zone temperature below the reference temperature:

$$UH = \sum_n \max\{0, R - T_Z\}. \quad (41)$$

We computed these coefficients on the same data range (5 days). In this way are the other model variables same so we do not have to consider their impact. The results are presented in the following table.

Type	TE	UH
ON-OFF controller	1025.3	106.994
PI controller (Mass flow)	1025.8	103.139
PI controller (Temperature)	1082.5	66.629
MPC-based controller	299.4	0

Table 5. Energy efficiency comparison.

From the energy efficiency point of view are the controllers of the supply fan mass flow almost the same. The difference between the consumed energy (TE) of the controllers

during the measured period is negligible. The PI controller was underheating only 3.6 % less than the on-off controller. The other benefit of the PI controller is that it never turns the fan completely off during the working time, so the fresh air is flowing into the zone all the time.

The PI controller of the supply air temperature had 5.5 % higher energy consumption than the systems with the controllers of the supply fan mass flow. On the other hand, the underheating was 35.4 % lower than the underheating with the PI controller of the supply fan mass flow.

Lastly, the MPC-based controller saved 70.8 % energy compared to the energy consumed by the on-off controller (the second best at the energy consumption) and it was not underheating at all. This results makes the MPC-based controller the best option among the controller designed in this thesis.

6. Conclusion

The mathematical models of both buildings of interest were obtained. The model for Building A was created on the basis of the fundamental theory of heat transfer. This model was too complex for controlling purposes, therefore it was simplified by reducing the number of equations and neglecting the nonlinearities of the model as well as the items with the insignificant impact on the zone temperature. We created 4 models for further comparison, including the simplest one - the linear model.

The models with different simplifications were identified from the same data. In order to maintain the objectivity, the same set of data was used for the comparison of these models. The results of comparing the models were very similar, with the linear model being the least precise one. The biggest improvement in accuracy was achieved by adding the radiations to the linear model, on the other hand the nonlinearities of the coefficients did not enhance the model significantly.

According to results, the best fitting model is the complete model. However, the linear model demonstrated the best accuracy-complexity ratio among the considered models. For control purposes are the simplest models preferred, due to their less complex structure. Because the accuracy of the linear model was satisfying, the best choice for contingent control design is the linear model.

The mathematical model of the heat transfer in the Building B was created on the basis of the simple mixed air equation. The full model was introduced along with other variations such as neglected variables and lowered system order.

The process of identification of the model parameters was almost identical with the one used in the case of Building A. The results of the basic models, that were influenced only by the outside temperature and the supply fan input, were insufficient. The best results in increasing the accuracy of the model were achieved by adding the variable that represented the temperature in the corridor and increasing the model order from the first to the second. On the other hand, including the influences of the rest of the surroundings did not improve the model accuracy radically. The last minor improvement was achieved by identifying the model from the data with the partially smoothed heated-air temperature. The fit value of the final model was 67.93%.

After considering above presented results, the model with the best result (Model 5 identified from data with smoothed T_S) was chosen for further process of creating the control system.

Two different approaches to regulation were considered. Firstly, presetting the supply air temperature and feedback controlling of the supply fan mass flow. In this case was the supply air temperature set according to the identified dependence on the outside temperature. With this approach, we designed two controllers: the on-off controller and the PI controller. We found out that their energy efficiency was almost same, but the PI controller was underheating less.

The second approach to regulation was to preset the supply fan mass flow and control the temperature of the supply air. We again designed two different controllers: the PI controller and the MPC-based controller. With the MPC-based control the supply fan mass flow was set to maximum at all times while with the PI control the mass flow

was switching between zero and maximum according to the schedule. The PI controller was in this case less energy efficient than the controllers of the supply fan mass flow, but it was noticeably better when it came to underheating. The MPC-based controller was the most advanced controller designed in this thesis. The results confirmed the expectations. The MPC-based controller was the most energy efficient and the least underheating one.

Appendix A.

Table of identified parameters for Building A

Model:	Eq. 20	Eq. 19	Eq. 18	Eq 17
r_1	10.7988	15.743	10.0453	20.2102
r_2	0	1.5e-05	11.1051	0.036966
p_2	0.0080006	0.022666	0.0061528	0.0091299
h_4	0.3445	0.34869	0.3046	0.15591
h_{44}	0.020666	0.017968	0.01908	0.010019
h_5	0.22253	0.70899	0.0003495	0.19644
p_1	0.0089246	0.01292	0.0083746	0.016539
h_S	204.1761	239.6743	48.3212	159.3387
h_C	52.8214	25.7339	30.6826	21.5733
c_1	0.0034602	0.0035847	0.0030636	0.0052664
c_5	0.063318	0.044608	0.043	0.066895
c_6	0.012957	0.0045743	0.013965	0.011268
c_8	0.020184	0.01357	0.022902	0.010852
s_1	1.6895	1.4315	0.85235	1.3333
s_5	0.0037208	0.0051304	0.0059001	0.0034253
k_{sc}	-	-	1.25e-05	0.090356
k_{cs}	-	-	6.2457	1.1617

Appendix B.

Table of identified parameters for Building B

Parameter name	Model 1	Model 2	Model 3	Model 4	Model 5
b_1	-	-	0.54990	0.48781	0.62007
b_2	0.99997	0.79396	0.44986	0.46923	0.30477
b_3	-	-	-	-	0.00652
b_4	-	-	-	0.00689	0.04033
b_5	-	-	-	-	0.00612
b_6	-	-	0.00023	0.00110	0.00054
b_7	-	0.05597	-	-	0.00592
b_8	-	0.10000	-	0.03477	0.01550
b_9	-	0.04963	-	-	0.00000
b_{10}	0.00001	0.00000	0.00000	0.00000	0.00000
b_{11}	0.00783	0.11277	0.01703	0.05244	0.06621

Bibliography

- [1] Bourhan Tashtoush, M. Molhim, and M. Al-Rousan. “Dynamic Model Of an HVAC System for Control Analysis”. In: *Energy* 30 (10 2005).
- [2] Siddharth Goyal and Prabir Barooah. “A Method for Model-reduction of Non-linear Thermal Dynamics of Multi-zone Buildings”. In: *Energy and Buildings* 47 (Apr. 2012), pp. 332–340.
- [3] E.H Mathews et al. “Developing Cost Efficient Control Strategies to Ensure Optimal Energy Use and Sufficient Indoor Comfort”. In: *Applied Energy* 66 (2 2000).
- [4] M. Zaheer-Uddin. “Energy Start-stop And Fluid Flow Regulated Control of Multizone HVAC Systems”. In: *Energy* 18 (3 1993).
- [5] M. Mossolly, K. Ghali, and N. Ghaddar. “Optimal Control Strategy For a Multi-zone Air Conditioning System Using a Genetic Algorithm”. In: *Energy* 34 (1 2009).
- [6] Zhuang Wu, Roderick V.N. Melnik, and Finn Borup. “Model-based Analysis and Simulation of Airflow Control Systems of Ventilation Units in Building Environments”. In: *Building and Environment* 42 (1 2007).
- [7] Qi Qi and Shiming Deng. “Multivariable Control of Indoor Air Temperature and Humidity in a Direct Expansion (DX) Air Conditioning (A/C) System”. In: *Building and Environment* 44 (8 2009).
- [8] S. Ginestet and D. Marchio. “Control Tuning of a Simplified VAV System: Methodology and Impact on Energy Consumption and IAQ”. In: *Energy and Buildings* 42 (8 2010).
- [9] Younggy Shin, Young Soo Chang, and Youngil Kim. “Controller Design for a Real-time Air Handling Unit”. In: *Control Engineering Practice* 10 (5 2002).
- [10] Guillermo Escrivá-Escrivá, Isidoro Segura-Heras, and Manuel Alcázar-Ortega. “Application of an Energy Management and Control System to Assess the Potential of Different Control Strategies in HVAC Systems”. In: *Energy and Buildings* 42 (11 2010).
- [11] Gongsheng Huang, Shengwei Wang, and Xinhua Xu. “A Robust Model Predictive Control Strategy for Improving the Control Performance of Air-conditioning Systems”. In: *Energy Conversion and Management* 50 (10 2009).
- [12] Rafael Alcalá et al. “Fuzzy Control of HVAC Systems Optimized by Genetic Algorithms”. In: *Applied Intelligence* 18 (2 2003).
- [13] Servet Soyguder and Hasan Alli. “An Expert System for the Humidity and Temperature Control in HVAC Systems Using ANFIS and Optimization with Fuzzy Modeling Approach”. In: *Energy and Buildings* 41 (8 2009).
- [14] Rahul L. Navale and Ron M. Nelson. “Use of Genetic Algorithms to Develop an Adaptive Fuzzy Logic Controller for a Cooling Coil”. In: *Energy and Buildings* 42 (5 2010).

- [15] M. Zaheer-uddin and G.R. Zheng. “Optimal Control of Time-scheduled Heating, Ventilating and Air Conditioning Processes in Buildings”. In: *Energy Conversion and Management* 41 (1 2000).
- [16] Manohar R. Kulkarni and Feng Hong. “Energy Optimal Control of a Residential Space-conditioning System Based on Sensible Heat Transfer Modeling”. In: *Building and Environment* 39 (1 2004).
- [17] Jianbo Bai, Shengwei Wang, and Xiaosong Zhang. “Development of an Adaptive Smith predictor-based Self-tuning PI Controller for an HVAC System in a Test Room”. In: *Energy and Buildings* 40 (12 2008).
- [18] Hamed Moradi, Majid Saffar-Avval, and Firooz Bakhtiari-Nejad. “Nonlinear Multivariable Control and Performance Analysis of an Air-handling Unit”. In: *Energy and Buildings* 43 (4 2011).
- [19] M. Barták. *Úvod do přenosových jevu pro inteligentní budovy*. Prague, Czech Republic: CTU Prague, 2010.
- [20] William S. Janna. *Engineering Heat Transfer*. Boca Raton, FL: CRC Press, 2000.
- [21] Mehdi Maasoumy et al. “Online Simultaneous State Estimation and Parameter Adaptation for Building Predictive Control”. In: *Dynamic System and Control Conference (DSCC 2013)*. Stanford, CA, USA, 2013.
- [22] Joseph Fourier. *Theorie Analytique de la Chaleur*. Paris: Firmin Didot Père et Fils, 1822.
- [23] M. Pčolka et al. *Economical Nonlinear Model Predictive Control for Building Climate Control*. 2013.
- [24] S.A. Klein et al. *TRNSYS: A Transient System Simulation Program*. 2010.
- [25] D.C. Sorensen et al. *MATLAB, version 8.2.0.701 (R2013b)*. Natick, Massachusetts: The MathWorks Inc., 2013.
- [26] D.C. Sorensen et al. *Simulink, version 8.2 (R2013b)*. Natick, Massachusetts: The MathWorks Inc., 2013.
- [27] Peter May-Ostendorp et al. “Model-predictive Control of Mixed-mode Buildings with Rule Extraction”. In: *Building and Environment* 46 (2 2011).